LIMNOLOGY and OCEANOGRAPHY

ASLO

Limnol. Oceanogr. 9999, 2023, 1–16

doi: 10.1002/lno.12293

Successful acclimation of marine diatoms *Chaetoceros curvisetus/pseudocurvisetus* to climate change

Ivna Vrana [1*], **Blaženka Gašparović** [1*], **Sunčana Geček** [1], **Jelena Godrijan** [1], **Tihana Novak** [1], **Snježana P. Kazazić** [2], **Marina Mlakar** [1], **Nataša Kužat** [3], **Martin Pfannkuchen** [3], **Daniela Marić Pfannkuchen** [3]

[1]Division for Marine and Environmental Research, Ruđer Bošković Institute, Zagreb, Croatia
[2]Division of Physical Chemistry, Ruđer Bošković Institute, Zagreb, Croatia
[3]Center for Marine Research, Ruđer Bošković Institute, Rovinj, Croatia

Abstract

Two main parameters that structure the marine ecosystem by affecting species distribution, abundance, community structure, timing of major life cycle events, and trophic state of the ecosystem are temperature and nutrient availability. Faced with climate change, eukaryotic plankton cope at multiple levels through physiological accommodation, adaptive evolution, shift in time and/or space of habitat, and/or community responses. Thirty-two years of our phytoplankton research indicate that *Chaetoceros curvisetus/pseudocurvisetus* adjust to climate change more successfully than the majority of the accompanying phytoplankton taxa in the mesotrophic part of the NW Adriatic Sea, the Mediterranean. While the abundance of the entire accompanying phytoplankton community has decreased significantly since 2003 (the period of the northern Adriatic warming and oligotrophication) compared to the previous period (1986–2003), the abundance of *C. curvisetus/pseudocurvisetus* remained unchanged, while its contribution to the community increased significantly. Accommodation strategies include a change in the timing of high abundance and blooms in the surface layer and successful blooming in the deeper layers during warm months. Apart from the observed in situ accommodation, physiological acclimation to warming may involve changes in photosynthesis, respiration, growth, and cell biochemistry. Here, we conducted laboratory experiments with *C. pseudocurvisetus* to investigate how warming affects its biochemical response through the fatty acid remodeling of phospholipid classes. Long-term field observations and short-term laboratory experiments suggest that marine diatoms *C. curvisetus/pseudocurvisetus* are potential global winners with the ability to acclimate/adapt to climate change.

The amount of solar energy absorbed by the atmosphere is increasing as a result of the increased amount of greenhouse gases. The seas and oceans are changing. Climate-related changes include increases in water temperatures, acidification, and deoxygenation, leading to changes in ocean circulation and sea level rise. Temperature is an important physical variable structuring the marine ecosystem and has a direct influence on the distribution and composition of marine species, community structure, species abundance, timing of major life cycle events, and the trophic state of the ecosystem (Richardson 2008). The availability of inorganic nutrients is an important chemical parameter affecting the global distribution, productivity, and size of phytoplankton (Behrenfeld et al. 2006). The Mediterranean Sea, including the northern Adriatic, is a hot spot in terms of sea temperature rise (Pastor et al. 2018). The consequences of exacerbating the effects of climate change on the Adriatic Sea are warming of seawater, an increase in salinity, and a decrease in phosphorus that are caused by the decrease in average annual rivers' discharges (Grilli et al. 2020).

One of the most important goals in marine research is to assess the potential impacts of global change stressors on biological communities (Mason et al. 2017). Marine primary producers

*Correspondence: ivna@irb.hr; gaspar@irb.hr

Additional Supporting Information may be found in the online version of this article.

Author Contribution Statement: I.V. and B.G. wrote the original draft while all other authors participated in reviewing and editing the manuscript. S.P.K., I.V., T.N., J.G., N.K., M.P. and D.M.P. performed the experiments, and analyzed the data. S.G. done statistical analysis. N.K., D.M.P. and T.N. undertook field sampling. B.G., M.M., J.G., M.P. and D.M.P. designed the study. B.G., M.M. and M.P. funding acquisition. All authors have read and agreed to the published version of the manuscript.
Special Issue: Cascading, interactive, and indirect effects of climate change on aquatic communities, habitats, and ecosystems.

are responsible for nearly half of the biosphere net primary production (Field et al. 1998). They are responsible for most of the flux of organic matter to both higher trophic levels and to deep waters (Falkowski et al. 2004). Faced with climate change, phytoplankton evolve mechanisms aimed at achieving cellular homeostasis via physiological and/or genetic changes through evolution. This also includes changes in the overall phytoplankton community composition (community response). The responses are more pronounced under nutrient-poor conditions (Filiz et al. 2020). Within phytoplankton, diatoms are the most abundant and ecologically most successful group, contributing for 27.7% of the total eukaryotic photosynthetic planktonic community (Malviya et al. 2016). They contribute up to 40% of the total ocean primary production (Nelson et al. 1995). Diatoms play important role in organic matter production and carbon cycling in the marine ecosystem (Obata et al. 2013). Among diatoms, the *Chaetoceros* genus is the most abundant and diverse group, accounting for 23.1% of all planktonic genera (Malviya et al. 2016; Busseni et al. 2020).

Marine lipids are a crucial component in a number of essential biological processes (Arts et al. 2001). They play an important role in the marine food web and also have health benefits for higher trophic levels including humans. Due to their heterogeneous nature, lipids are great biogeochemical markers for tracking the adaptation of marine species to different environmental conditions, trophic markers in food webs, and for identifying different sources and processes of marine organic matter (Parrish et al. 2000; Guschina and Harwood 2009). Phospholipids (PL), including phosphatidylcholines (PC), phosphatidylinositols (PI), phosphatidylethanolamines (PE), phosphatidic acids (PA), and phosphatidylserines (PS), are important structural membrane lipids that serve diverse roles in the cell (van Meer et al. 2008). Phosphatidylglycerols (PG) are the only PL found in detectable amounts in thylakoids. Each PL class contains a variety of molecular species that are distinguished by the length and degree of saturation of their acyl chains. Cellular organelles have lipid compositions that are suited to their specific functions. These parameters must be kept within a certain range for the proper function because even small changes in lipid composition can have a big impact on membrane properties and the associated processes. The physical properties of the membrane are influenced by both the head group and the acyl chain composition (Holthuis and Menon 2014). Class-level analysis of PLs is critical to understanding the adaptive mechanisms of phytoplankton to various environmental stresses (Popendorf et al. 2011). PL content in phytoplankton can vary considerably, from a few percent to 61% of total lipid content (Guschina and Harwood 2009; Artamonova et al. 2017).

Here, we analyzed the long-term distribution of *Chaetoceros curvisetus/pseudocurvisetus* and the total accompanying eukaryotic phytoplankton in the Mediterranean coastal region (the NW Adriatic), over a period from 1986 to 2017. During regular monthly monitoring of the phytoplankton community in the northern Adriatic Sea it was observed that in 2010 there was large contribution of *C. curvisetus/pseudocurvisetus* in the total phytoplankton community (J. Godrijan pers. comm.). This observation, together with the fact that the northern Adriatic is already recognized as a sea that changes relatively rapidly under the influence of global change (*Estuarine, Coastal and Shelf Science*, vol. 115), motivated us to conduct a comprehensive analysis of *C. curvisetus/pseudocurvisetus* and the accompanying phytoplankton. Because of the difficulty in distinguishing between *C. curvisetus* and *C. pseudocurvisetus* under the light microscope, data are presented as *C. curvisetus/pseudocurvisetus*. We performed analyses to determine temporal changes in the abundance of *C. curvisetus/pseudocurvisetus*, total accompanying phytoplankton community and resulting changes in *C. curvisetus/pseudocurvisetus* community share. We tested their possible seasonal changes in abundance in relation to earlier and recent periods and changes in depth distribution. We hypothesized that *C. curvisetus/pseudocurvisetus* might change their temporal blooming preferences as a result of environmental changes. Because the two most important parameters structuring phytoplankton community are temperature and nutrient availability (here studied trough salinity changes), we analyzed the relationships between temperature and salinity variables (in the form of anomalies) and *C. curvisetus/pseudocurvisetus* occurrences, and *their* community share. Finally, we hypothesized that *C. curvisetus/pseudocurvisetus* are accommodating to the observed changes in the region.

To complete the knowledge of possible mechanisms of accommodation, it is important to investigate possible acclimation/s at the cellular level (changes in photosynthesis, respiration, growth, and cell biochemistry) in addition to adaptation in situ. Therefore, we performed a controlled laboratory cultivation of *C. pseudocurvisetus* at five temperatures: 10°C, 15°C, 20°C, 25°C, and 30°C, covering the annual temperature range of the northern Adriatic Sea, under conditions of high nutrient content. We studied its survival and PL fatty acid (FA) remodeling caused by warming. We hypothesized that *C. pseudocurvisetus* would remodel PL under warming conditions as one of the possible acclimation mechanisms to increasing temperature. This is because the cell membrane, which among other things serves to protect and organize the cell and is composed mainly of PLs, is the first to perceive environmental changes. Studies aimed at understanding future changes in phytoplankton communities as a result of global warming have focused on physiological traits, including temperature-induced changes in growth rate, and photosynthesis and respiration (Huertas al. 2011; Jin and Agusti 2018; Schaum et al. 2018). Our data are the first report of physiological acclimation through PL FA remodeling as a result of *C. pseudocurvisetus* short-term response to temperature stress.

Methods

Field study

The study was conducted in the NW Adriatic (Mediterranean) at two stations, meso- to eutrophic stations

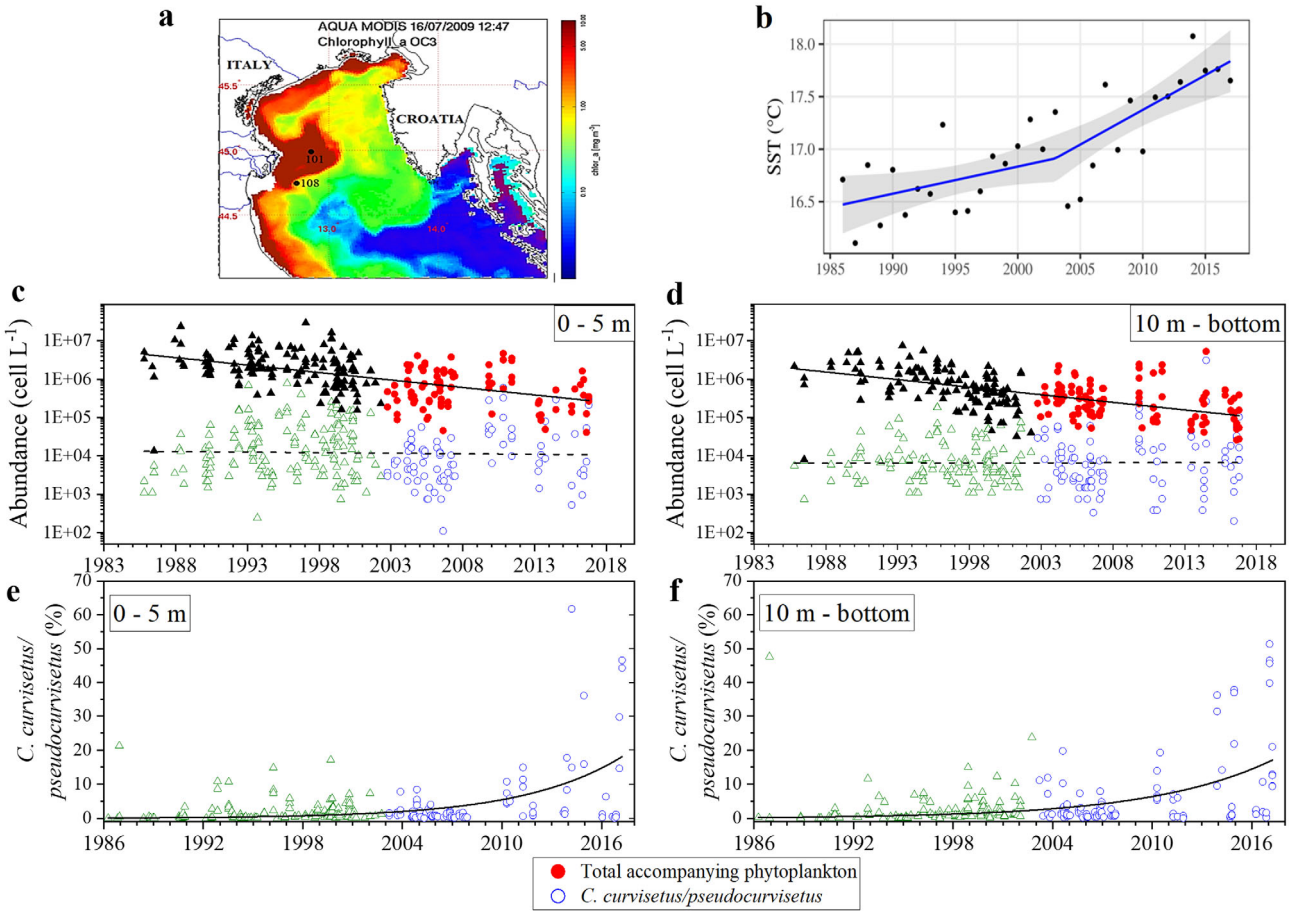

Fig. 1. Long-term (1986–2017) data on phytoplankton in the NW Adriatic Sea. (**a**) The northern Adriatic chlorophyll *a* data derived from MODIS full resolution data from 16 July 2009. This figure shows the influence of high Po River nutrient load on enhanced phytoplankton blooms at the NW Adriatic. Marked are sampling stations. (**b**) Average Sea surface temperature (SST) (blue line). The gray area around the blue trend line indicates the 95% confidence interval. (**c**, **d**) Abundance of total accompanying phytoplankton (linear fits, solid lines, $p < 0.001$) and *Chetoceros curvisetus*/*pseudocurvisetus* (non-significant, dash lines). (**e**, **f**) The relative contribution of *C. curvisetus*/*pseudocurvisetus* (exponential fits, solid lines, $p < 0.001$). Data are represented separately for years 1986–2002 by triangles and for years 2003–2017 by circles and for two water column layers ((**c**, **e**) surface 0–5 m depth that is more influenced by warming and higher salinity with respect to less influenced (**d**, **f**) deeper layers, 10 m to bottom). Full symbols represent total accompanying phytoplankton data while open symbols *C. curvisetus*/*pseudocurvisetus* data.

101 (44°59′53″N, 12°49′48″E) and 108 (44°45′24″N, 12°45′0″E), which are influenced by the Po River (Fig. 1a). The NW Adriatic Sea is the northernmost part of the Mediterranean Sea. It is shallow with a maximum water depth of 30 m. Due to nutrient input from the River Po, it is an area of high productivity (Ivančić et al. 2012). The most important factor affecting biogeochemical processes is the Po River, which dilutes seawater and brings high NO_3^- (ranging 128–202 μmol L^{-1}) and PO_4^{3-} (ranging 1.3–2.6 μmol L^{-1}) loads (Cozzi and Giani 2011). In addition, there are physical parameters such as the regular seasonal light cycle, the annual temperature cycle, and the surface currents that influence the distribution of biological productivity in the region (Solidoro et al. 2009). In winter, river water is directed southward due to the prevailing cyclonic Adriatic circulation in the narrow coastal belt. During the stratification of the water column in the warmer season, a countercurrent occurs, called the Istrian Coastal Countercurrent (Supić et al. 2000). This anticyclonic current transports low salinity water to the eastern part of the northern Adriatic.

Samples were taken from April 1986 to August 2017 at depths of 0.5, 5, 10, 20 m, and the bottom (~ 30 m) using Niskin bottles from the RV "Vila Velebita." In parallel to sampling, temperature and salinity were measured using a CTD probe (Seabird SBE25, Sea-Bird Electronics Inc.). The sampling cruises were conducted under the auspices and with the permission of the Croatian Ministry of Environmental Protection and Energy. Seawater samples for phytoplankton analysis were filtered through a 300 μm mesh plankton net immediately after collection. Phytoplankton samples (200 mL) were preserved in 2% (final concentration) formaldehyde neutralized with disodium tetraborate decahydrate, stored in a cool and dark conditions and analyzed within 1 month after sampling.

Quantitative and qualitative phytoplankton analysis

The spatial and temporal distribution of phytoplankton was extracted from a long-term monitoring dataset containing two sampling locations (Stas. 101 and 108) with approximately monthly sampling frequencies between 1986 and 2017. Subsamples of 50 mL for phytoplankton analysis were gently homogenized and sedimented for 40 h and analyzed using a Zeiss Axiovert 200 microscope following the Utermöhl method (Utermöhl 1958). Phytoplankton cells were identified and counted in random fields under ×400 and/or ×200 magnification. The total phytoplankton abundance includes all species counted in the microphytoplankton (20–200 μm) and nanophytoplankton (2–20 μm) groups (Sieburth et al. 1978). Phytoplankton were determined at the species level whenever possible, using standard keys and manuals (Schiller 1937; Tomas 1995). The accuracy of the counting method is ± 10% (Utermöhl 1958). During the studied period, there were numerous changes in taxonomy, so we updated the species list before starting the biodiversity analyses. No taxonomic analysis was conducted in 2008, 2009, 2012, and 2015, and there was no sampling in May of the entire 2003–2017 period due to regular annual maintenance of the research vessels. Here, we elaborated a dataset of 468 samples in which *C. curvisetus*/*pseudocurvisetus* were found.

Species isolation and culture condition setup

Since a large share of *C. curvisetus*/*pseudocurvisetus* in the total phytoplankton community in the northern Adriatic in the 2010 s was observed (J. Godrijan pers. comm.), a *C. pseudocurvisetus* colony was manually isolated with a micropipette from a net sample at 20 m depth (17.08°C) in October 2014 at Sta. 101 (Fig. 1a). We maintained the monoclonal batch culture in 100 mL of *f*/2 medium (Guillard 1975) in sterile VWR tissue culture flasks (VWR) at 15°C and 4500 lx, with a 12 : 12 h light/dark photoperiod, and subcultured it every 2–3 weeks until May 2015, corresponding to approximately 90 generations, when the cultivation experiments started. The culture's genetic material is deposited in GenBank under Accession numbers MG385841 (18S DNA) and MG385842 (28S DNA). The media was prepared using seawater from the northern Adriatic Sea, stored in the dark for 2 months, filtered through sterile 0.22 μm white plain filters (Merck Milipore Ltd.), and boiled in the microwave. Media amendments were added aseptically after sterilization. Cultivation was performed at five temperatures: 10°C, 15°C, 20°C, 25°C, and 30 ± 0.1°C. This temperature range represents the typical annual temperature range in the northern Adriatic Sea (Gašparović 2012). The average initial orthophosphate (PO_4^{3-}) concentration was 36.33 ± 6.56 μmol L^{-1}. Dissolved inorganic nitrogen (DIN = $NO_3^- + NO_2^- + NH_4^+$) concentrations were 1059 ± 181.1 μmol L^{-1}. We started the experiment with 1×10^5 cells L^{-1} in 800 mL sterile cell culture flasks (Corning Inc.) in a thermostatic chamber (Inkolab) with 12/12 h light/dark cycle under the illumination of ~ 4500 lx. The light source was white LED whose spectral irradiance (OceanOptics HR4000 High-Resolution Fiber Optic Spectrometer) in the chamber is shown in Fig. S1. Cultures were mixed manually twice a day. Cells were harvested on the third day of the stationary phase: days 17, 11, 9, 11, and 10 for cultivation temperatures of 10°C, 15°C, 20°C, 25°C, and 30°C, respectively. Nutrients were not limiting at the end of cultivation. Growth phase was determined by counting cells every other day using the Fuchs-Rosenthal chamber under an Olympus BX51-P (Olympus) polarizing microscope. All experiments were performed in duplicate. Before the experiment, *C. pseudocurvisetus* cells were preconditioned to the experimental temperature in a 50 mL cell culture flask for 2 weeks, which was between 3.5 and 9 generations depending on the temperature.

Lipid extraction and analysis

Diatom cultures (100 mL) were filtered through 0.7 μm Whatman GF/F filters (preburned at 450°C for 5 h) and the filters were stored at −80°C until analysis. Particulate lipid extraction was performed using a modified method of Bligh and Dyer (1959). Briefly, 10 mL of monophasic solution (dichloromethane/methanol/deionized water, 1 : 2 : 0.8 vol/vol/vol) and 10 μg of the standard *n*-nonadecanone were added to the sliced filters in the cuvettes. They were then sonicated for 3 min, stored overnight at 4°C, filtered through a sinter funnel into a separatory funnel, washed again with 10 mL of monophasic solution, and then with 10 mL of biphasic solution (dichloromethane/ 0.73% NaCl, 1 : 1 vol/vol). Lipids in dichloromethane were collected and the extraction was repeated with 10 mL of dichloromethane. *N*-nonadecanone was added to each sample as an internal standard to estimate recoveries in subsequent steps of sample analysis. Extracts were evaporated to dryness under nitrogen flow and dissolved in 20–50 μL dichloromethane (Merck) (arbitrarily determined based on the researcher experience).

Thin-layer chromatography with a flame ionization detector was used to determine the lipid classes. The lipid content determined by this method is close to the values determined gravimetrically (Parrish 1987). Eighteen lipid classes were separated on Chromarods SIII and quantified by external calibration with a standard lipid mixture using the Iatroscan MK-VI (Iatron) with a hydrogen flow of 160 mL min^{-1} and an air flow of 2000 mL min^{-1}. Lipid calibrations were performed based on 10–16 concentrations covering a range of 0.2 to 5.0 μg. Data (peak area vs. mass [in μg]) were fit with power functions. Sample aliquots (2 μL) in dichloromethane were spotted using a semiautomatic sample spotter. Each lipid extract was analyzed in duplicate. The standard deviation determined from the duplicate runs accounted for 3–11% of the relative abundance of the lipid classes. The separation scheme for all classes included seven elution steps in solvent systems of increasing polarity. PL separation included three classes: PC, PG, and PE. PS, PA, and PI co-elute with PC, PG,

and PE. Protocols for them are not included due to too high detection limits. PG were separated with the solvent mixture acetone–chloroform–methanol–formic acid (33 : 33 : 33 : 0.6, vol : vol : vol : vol) for 40 min. The solvent mixture chloroform–methanol–ammonium hydroxide (50 : 50 : 5, vol : vol : vol) for 30 min allowed PE and PC separation. The detailed procedure for all 18 classes is described in Gašparović et al. (2015). Total lipid concentration was calculated as the sum of all detected lipid classes, while total PL concentration was calculated as the sum of PG, PE, and PC.

High-performance liquid chromatography (UltiMate 3000 RSLC; Dionex) electrospray ionization (tandem) mass spectrometry (amaZon ETD; Bruker Daltonik) was used for PL molecular identity determination. Mobile phase A was LC-MS grade methanol: ultrapure water (1 : 1 vol/vol with 10 mmol L^{-1} ammonium acetate and 0.1% formic acid) and mobile phase B was LC-MS grade isopropanol (with 10 mmol L^{-1} ammonium acetate and 0.1% formic acid). The gradient was used as follows: 55% A/45% B at the beginning, reaching 90% B in 40 min, 99% B in 2 min (hold 10 min), then back to 45% B in 1 min, and equilibrate for 22 min for the next injection. An Acquity UPLC BEH C18 column (Waters) with a 2.1 mm × 100 mm ID and 1.7 μm particles size was used. The column oven and the flow rate were 50°C and 0.15 mL min^{-1}, respectively. Before injection (10 μL), dichloromethane was evaporated from the samples (after TLC analysis) and dissolved in methanol : chloroform (1 : 2, vol : vol) solution. Depending on the sample, between 4.0 and 17.5 μg of the lipids were injected. Mass spectrometric detection was performed using a standard ESI ion source (nebulizer pressure 8 psi; drying gas flow rate 5 L min^{-1}; drying gas temperature 250°C; the potential on the capillary ± 4500 V) operated in positive and negative modes. The PLs classes PG, PE, PI, PA, and PS were identified as $[M - H]^-$ ions in the negative mode, whereas PC was identified as $[M + H]^+$ ions in the positive mode. The data were collected in a mass range of m/z = 100–1200 and the collision energy was set to 1 eV. Data were collected using DataAnalysis software (Bruker Daltonik) and analyzed using a self-developed computer programme derived from LIPID MAPS that allows identification of the lipid species analyzed. In-house written code was compiled using the Microsoft C# compiler in Visual Studio (Microsoft). The parameters were set as follows: retention time 2.05–40 min, mass tolerance at 0.05 Da, and retention time tolerance at 0.1 min.

PL classes' composition is discussed in the terms of the diversity of PL molecular species. We present even PL FA profiles, ranging from 14 to 22 carbon atoms (C14–C22).

Statistical methods

Statistical analysis of field data

Statistical analyses and graphical representation of results were performed in the R statistical environment (R version 3.6.3, R Studio 1.2.5033; R Core Team 2020). Data are analyzed separately for the period before (1986–2002) and after the major warming of the northern Adriatic (2003–2017). The data are also interpreted for two layers: the surface (0.5–5 m depth) and the deeper, colder (10 m to the bottom [~ 30 m]) layer (Gašparović 2012). The *base* (R Core Team 2020) and *pastecs* packages (Grosjean and Ibanez 2018) were used for descriptive statistics and basic homoscedasticity (Levene's test), normality (Shapiro–Wilk test, QQ-plot), and extreme value tests, whereas the *ggplot2* package (Wickham 2016) was used for graphical presentation. A significance level of 0.05 was used for all statistical analyses unless otherwise stated.

Temporal changes in environmental variables were examined using data from the Copernicus Marine Service (CMEMs). Satellite measurements of sea surface temperature (SST) were obtained for coordinates 44.88°N and 12.79°E from the *cmems_SST_MED_SST_L4_ REP _OBSERVATIONS_010_021* dataset. Daily and monthly means for temperature in the deeper layer (19 m depth, T_{Re}) and salinity in both layers (1 and 19 m depth, S_{Re}) were obtained for the same site from the *MEDSEA_MULTIYEAR_PHY_006_004* reanalysis dataset. We used the *Splines* package in R (Bates and Venables 2020) to fit piecewise linear splines to the annual mean SST values in the surface layer to confirm the increase in temperature over time. The difference in annual mean temperatures between two time periods (1986–2002 and 2003–2017) and layers (surface and deeper layer) was examined using factorial robust Anova (factors: time period, layer). Robust Anova based on trimmed means (20% of trimming level; *WRS2* package in R: Mair and Wilcox 2020; Wilcox 2012) were used instead of classical ANOVAs to overcome the problems associated with deviations from homoscedasticity and to reduce the influence of outliers observed in the data. Post hoc tests were also performed in the robust *WRS2* environment, while p values were adjusted for multiple testing using the Benjamini-Hochberg (BH) method. The *multcompView* package (Graves et al. 2019) was used to convert the vector of p values to a character-based representation in which common characters denote levels or groups that are not significantly different.

Annual trends in abundance/community share of *C. curvisetus/pseudocurvisetus* and abundance of total accompanying phytoplankton were examined using regression analysis in R (linear model, *lm* routine). Data were log-transformed (base *e*) and grouped annually prior to analysis to stabilize variances, obtain an approximately normal distribution of residuals, and filter out seasonal cycles from the data. Seasonal patterns by time period (1986–2002 and 2003–2017) and layers (surface and deeper layer) of *C. curvisetus/pseudocurvisetus* abundance/community share and total accompanying phytoplankton abundance were assessed using a linear mixed effects (LME) model. For each season, two fixed effects were incorporated into the model (time period and layer) to account for the change in the dependent variable between periods and layers, while the random effect (years)

was incorporated to account for the repetition of measurements within a year/season. The mixed effects model was built in R using the *lme4* package (optimizer: *bobyqa*) (Bates et al. 2015). ANOVA for an unbalanced design (type III) was used to estimate the significance of fixed effects. A comprehensive report on the statistical methods used to analyze the LME model results can be found at the end of the Supporting Information document. Phenology of *C. curvisetus*/*pseudocurvisetus*, that is, temporal shifts in succession at a monthly scale, were examined by post hoc Tukey test (*TukeyHSD* on *aov* from the R *base* package).

To determine the relationship between the occurrence/abundance of *C. curvisetus*/*pseudocurvisetus* and environmental variables on a longer temporal scale, we used anomalies instead of baseline variables to filter out the variance in the annual cycle and intra-annual relationships. Because estimating anomalies required data sampled at higher frequencies, we incorporated SST data and temperature and salinity values from the CMEMS reanalysis dataset in the analysis. Monthly temperature and salinity anomalies and 10-d average anomalies were calculated with respect to the 1985–2002 mean monthly climatology. The *Splines* package in R (Bates and Venables 2020) was used to confirm the increase in anomalies over time. For boxplots of monthly anomalies, 95% confidence intervals were calculated using the Wilcoxon rank-sum test.

To test whether the temperature and salinity anomalies when *C. curvisetus*/*pseudocurvisetus* was detected in the second period 2003–2017 were the same as in the first period 1986–2002, robust factorial Anova (factors: time period, layer) based on trimmed means (20% of trimming level), post hoc tests, and adjustment of p values according to the BH were performed in the robust *WRS2* environment (Mair and Wilcox 2020). To assess whether the effects of the shift in environmental variables on the *C. curvisetus*/*pseudocurvisetus* community share differed between the two time periods, a linear model *lm (Comunity share* ~ *Period*Temperature anomaly* + *Period*Salinity anomaly)* was constructed in R for both layers, after the three-way interaction *period*temperature anomaly*salinity anomaly* was confirmed to be not significant. ANOVA for an unbalanced design (type III) was used to estimate the significance of the effects.

Statistical analysis of lipidomics data from laboratory experiments

Linear and polynomial fits (computer software Origin 7, Origin Lab) were performed to examine the possible temperature effect on the *C. pseudocurvisetus* PL characteristics including average number of molecular species, average PL fatty acyl chain length, and average fatty acyl chain double bonds. A polynomial fit was performed when the highest or lowest values were found at intermediate temperature corresponding to the optimal growth temperature (15°C). In these cases, the linear fit would result in unrealistic values for the relationship between temperature and certain PL parameters. Post hoc Tukey tests *TukeyHSD* on *aov* from the R base packages (R Core Team 2020) were performed to determine the significance of all temperature combinations-related changes in lipid/PL contents and PL characteristics (molecular diversity, acyl chain length, acyl double bonds).

Results

Long-term investigations of *C. curvisetus*/*pseudocurvisetus* in the NW Adriatic Sea

Long-term data over 32 years on eukaryotic phytoplankton included taxonomy and abundances. Since we were interested in the effects of climate change on eukaryotic plankton and wanted to distinguish between the two main influences of warming and oligotrophication observed for the northern Adriatic (Gašparović 2012), we chose the meso- to eutrophic NW Adriatic as sampling site (Fig. 1a). In this way, we wanted to avoid conditions where severe nutrient deficiency affects phytoplankton abundance, community composition and seasonal cycle, as observed in the NE Adriatic (Marić et al. 2012).

Since 2003, average annual SST in the region has increased significantly (Fig. 1b) (piecewise-linear spline fit, $R^2 = 0.66$, $F(2, 29) = 28.05$; $p < 0.001$), with extreme in situ temperatures often reaching or exceeding 30°C in summer (e.g., Novak et al. 2018). The significant overall increase in temperature between two periods (1986–2002 and 2003–2017) was confirmed by a factorial robust ANOVA (factors: period, layer) of annual temperatures estimated from the CMEMs reanalysis dataset (Fig. S2a; Table S1a,b). The slight increase in salinity values, an indication of less nutrients, in the later period was also observed (Fig. S2b; Table S1a,b). The increase in both environmental variables was more pronounced in the surface than in the deeper layer (robust post hoc analysis; Table S1c). The slightly higher seawater salinity in the later period is a consequence of the reduced inflow of the Po River freshwater which is related to the shortening of the snow cover in the Italian Alps (Gašparović 2012).

Here, we present data for samples in which *C. curvisetus*/*pseudocurvisetus* were found (Fig. 1c–f). To understand whether *C. curvisetus*/*pseudocurvisetus* have acclimated/adapted to the observed changes in the northern Adriatic (*Estuarine, Coastal and Shelf Science*, vol. 115) compared to sympatric species, we present data on the abundance of the total phytoplankton that accompanied *C. curvisetus*/*pseudocurvisetus* (Fig. 1c,d), as well as the abundance (Fig. 1c,d) and relative contributions of *C. curvisetus*/*pseudocurvisetus* to the community (Fig. 1e,f).

Temporal changes in abundances of *C. curvisetus*/*pseudocurvisetus* and accompanying phytoplankton are shown in Fig. 1c,d. Abundance of total accompanying phytoplankton decreased significantly with time, both at the surface (Figs. 1c, S3a; Table S2) and in the deeper layer (Figs. 1d, S3b; Table S2). In contrast, *C. curvisetus*/*pseudocurvisetus* abundance did not decrease significantly (Figs. 1c,d, S3c,d; Table S2), resulting in

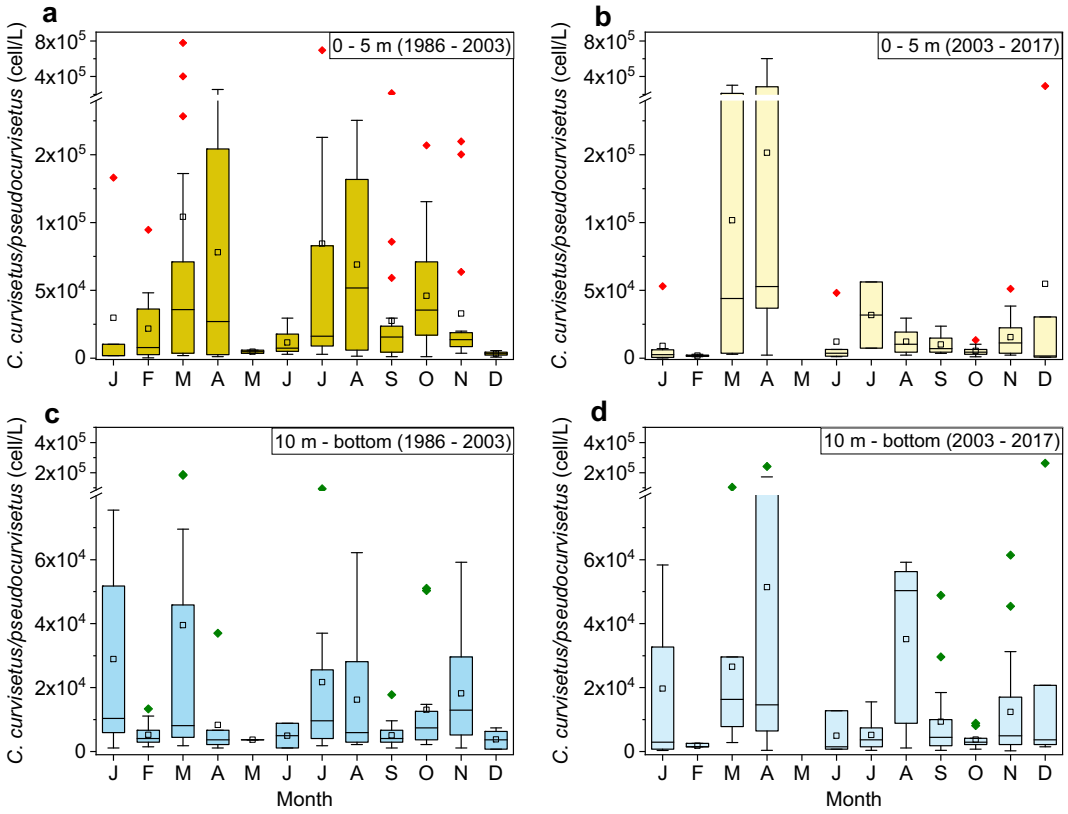

Fig. 2. *Chaetoceros curvisetus/pseudocurvisetus* timing of high abundance and blooms throughout the annual cycle. Data are presented for the two periods (**a**) and (**c**) earlier colder period from 1987 to 2003 and (**b**) and (**d**) later warmer period from 2003 to 2017 and two water column layers ((**a**, **b**) surface 0–5 m depth that is more influenced by the warming with respect to less influenced (**c**, **d**) deeper layers, 10 m to bottom). The box in the box and whisker plots is determined by the 25th and 75th percentiles, the whiskers are determined by the 5th and 95th percentiles, squares correspond to means, horizontal lines correspond to medians, rhombus correspond to outliers.

an increase in the *C. curvisetus/pseudocurvisetus* community share over time (Figs. 1e,f, S3e,f; Table S2).

Seasonal patterns across periods and depths are statistically processed by LME model and presented in Tables S3–S5. Abundance of total accompanying phytoplankton significantly decreased during the later period 2003–2017 in all seasons (Table S3a,b), with a 2.3- to 5.4-fold decrease in seasonal mean values. Their abundance was significantly higher in the upper layer from spring to autumn (Table S3). No difference between the layers in winter is due to the fully vertically mixed water column. A significant difference in *C. curvisetus/pseudocurvisetus* abundance between the two periods was observed only in autumn (2.0-fold decrease in autumn) (Table S4a,b). The seasonal depth distribution of *C. curvisetus/pseudocurvisetus* was similar to that of the accompanying phytoplankton (Table S4).

As a result of the seasonal dynamics of *C. curvisetus/pseudocurvisetus* and associated phytoplankton, the community share of *C. curvisetus/pseudocurvisetus* differed significantly between two periods in spring (8.7-fold increase in means in the later period) and winter (1.9-fold increase in means in the later period) (Table S5). Vertically, a significant difference in *C. curvisetus/pseudocurvisetus* community share between two layers was observed in summer with a lower community share in the surface in relation to the deeper layer (Table S5) when the water column is highly stratified.

We were interested in whether there was *C. curvisetus/pseudocurvisetus* temporal succession shift(s) during the later warmer and somewhat less nutrient rich period characterized by higher salinity (Fig. 2). In the first period (1986–2002) during a year, increased abundances were found in the surface layer in March, April, August, and October (Fig. 2a). In the later period (2003–2017) during a year, increased abundances of *C. curvisetus/pseudocurvisetus* were observed in surface waters in March and April (Fig. 2b). The disappearance of high abundances of *C. curvisetus/pseudocurvisetus* in the surface layer in August and October is statistically confirmed by the post hoc Tukey test (Table S6). Cell concentrations of *C. curvisetus/pseudocurvisetus* higher than > 10^5 cell L^{-1} in the surface layer were observed in the first period from January to November (in 12.8% of samples), while in the second period such cell concentrations were observed in 6.8% of samples in May,

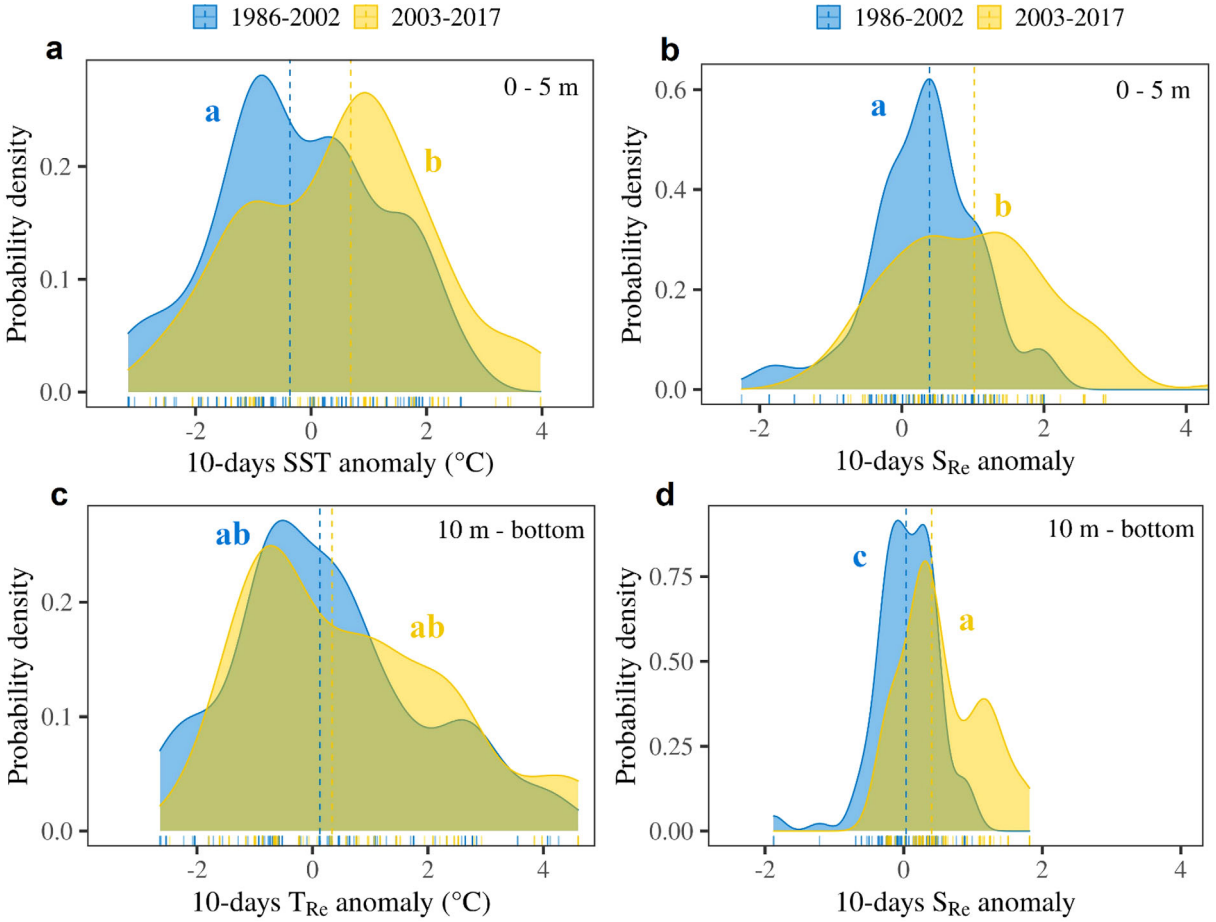

Fig. 3. Probability distribution for 10-d averaged anomalies of temperature and salinity values present when *C. curvisetus/pseudocurvisetus* were found in the phytoplankton community: (**a**) 10-d average of SST anomaly of the surface layer; (**b**) 10-d average of salinity anomaly (S_{Re}) of the surface layer; (**c**) 10-d average of temperature anomaly (T_{Re}) of the deeper layer; (**d**) 10-d average of salinity anomaly (S_{Re}) of the deeper layer. Ten-day average of temperature and salinity anomalies are calculated with respect to the mean monthly 1985–2002 climatology. Dashed lines represent median sample values. Significant differences between periods and layers for pair of panels **a**/**c** and **b**/**d**, are marked with different letters.

April, and December. Deeper layers did not differ in high abundances of *C. curvisetus/pseudocurvisetus* between the two periods (Fig. 2b,d; Table S6). However, *C. curvisetus/pseudocurvisetus* cell concentrations > 10^5 cell L^{-1} in the deeper layer were observed in the first period in 1.6% of the samples and only in March, while in the second period in the 5.6% of the samples abundances greater than 10^5 cell L^{-1} were observed in March, April, and December, with an extreme value of 3×10^6 cell L^{-1} in December 2014.

We investigated the relationships between environmental variables and the occurrence of *C. curvisetus/pseudocurvisetus*. To do this, we chose to work with temperature and salinity anomalies. The temperature anomaly was chosen instead of temperature to filter out variance in the annual temperature cycle and intra-annual relationships. We used 10-d anomalies because this is the optimal span between cell growth (2–3 d) and community turnover (2 weeks) (Bosak et al. 2016). Because a positive temperature anomaly was found in the later period 2003–2017 (Fig. S4b,f), we were interested in the following questions: (1) did *C. curvisetus/pseudocurvisetus* adjust their occurrence to the temperature shift, or were the temperature anomalies at which *C. curvisetus/pseudocurvisetus* were detected in the later period 2003–2017 the same as in the first period 1986–2002, and (2) did the effects of the shift in environmental variables on the *C. curvisetus/pseudocurvisetus* community share differ between the two periods? During 2003–2017, *C. curvisetus/pseudocurvisetus* were detected at higher 10-d temperature anomalies in the surface layer (0–5 m depth) (Fig. 3a; Table S7). Positive salinity anomalies were detected for the surface and deeper layers in the later period compared to the earlier period (Fig. S5), indicating lower nutrient input lately. In both layers, *C. curvisetus/pseudocurvisetus* were observed at higher salinity anomalies during the 2003–2017 period (Fig. 3b,d; Table S7).

The effects of the anomaly of environmental variables on the *C. curvisetus/pseudocurvisetus* community share were

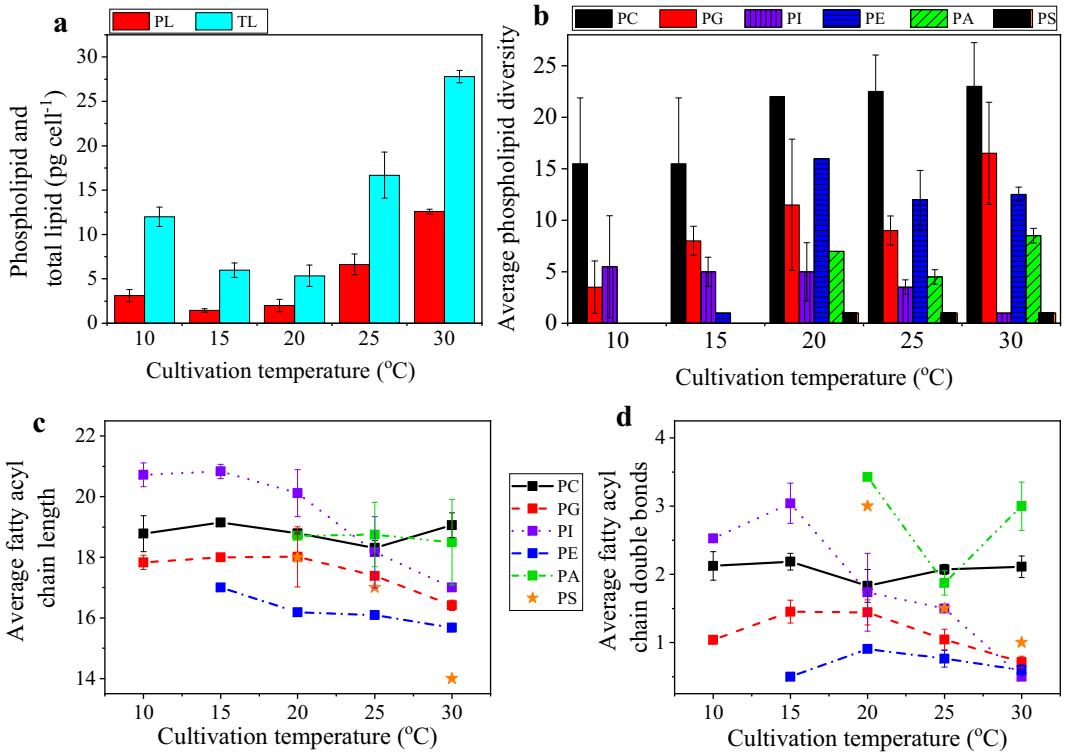

Fig. 4. Diatom *Chaetoceros pseudocurvisetus* lipid production and average characteristics of phosphatidylcholines (PC), phosphatidylglycerols (PG), phosphatidylinositols (PI), phosphatidylethanolamines (PE), phosphatidic acids (PA), and phosphatidylserines (PS). (**a**) The average phospholipid and total cell lipid (TL) cell concentration (pg cell^{-1}) ± SD. (**b**) The average phospholipid diversity (the number of molecular species). (**c**) The average phospholipid fatty acyl chain length (number of acyl carbon atoms), and (**d**) the average fatty acyl chain double bonds. Error bars are the SD of two replicates. Probability values (*p* values) for all temperature combinations relating differences in lipid and phospholipid contents, and phospholipid characteristics (average number of molecular species, average phospholipid fatty acyl chain length and average fatty acyl chain double bonds) (post hoc Tukey test) are given in Table S9. The Tukey tests showed significant differences for all instances where average values differed more than accumulated standard deviations.

different in the two periods (Table S8). The positive SST anomalies observed for the surface layer supported the increase in community share in the later period 2003–2017 in contrast to the 1986–2002 period. This effect is not visible in the deeper layer. In the deeper layer, the increase in salinity anomaly (lower nutrient levels) was accompanied by a decrease in community share in the later period. However, the results of the analysis in the deeper layer should be interpreted with caution because they are based on estimated temperature and salinity values from the CMEM reanalysis rather than direct measurements, as is the case for SST.

C. pseudocurvisetus phospholipidomics

In situ data suggest that *C. curvisetus*/*pseudocurvisetus* successfully accommodate to the observed changes in the northern Adriatic. Therefore, their acclimation/adaptation at the cellular level can be expected, including physiological acclimation by changes in photosynthesis, respiration, growth, and cell biochemistry. Because *C. curvisetus*/*pseudocurvisetus* were detected in the later period at positive salinity anomalies, suggesting that fewer nutrients at higher salinities did not negatively affect their abundance, we conducted laboratory experiments to investigate the short-term *C. pseudocurvisetus* accommodation capacity with respect to its ability to adjust membrane PL composition under temperature increase. *C. pseudocurvisetus* was grown at five different temperatures. The highest cell abundance was observed at 15°C ($25.8 \pm 11.7 \times 10^6$ cell L^{-1}), and nine times lower at 30°C ($2.8 \pm 11.7 \times 10^6$ cell L^{-1}), while growth rates were lowest at 10°C (0.26 ± 0.03) and highest at 25°C (0.72 ± 0.03 d^{-1}) (Fig. S6) (Novak et al. 2019).

Higher growth temperatures (25°C and 30°C) resulted in significant accumulation of cell lipids ($p < 0.001$; Table S10) (16.7 ± 2.6 and 27.8 ± 0.7 pg cell^{-1}, respectively), including PL ($p < 0.001$; Table S10) (6.6 ± 1.2 and 12.6 ± 0.3 pg cell^{-1}, respectively), accumulation (Fig. 4a; Table S11).

Three lipid classes were detected at all temperatures: PC, PG, and PI, while PE, PA, and PS were detected at higher growth temperatures (Fig. 4b; Table S11). Greater PL molecular diversity was detected at higher temperatures for PC ($p = 0.043$; Table S10), PG ($p = 0.014$; Table S10), PE ($p < 0.001$; Table S10), and PA ($p = 0.001$; Table S10). The lowest total PL diversity was detected when *C. pseudocurvisetus* was growing at 10°C. At all cultivation temperatures, the

highest molecular diversity was found for PC, 16–25 species, and the lowest for PS (1 species; Fig. S13).

In general, PG ($p = 0.021$; Table S10), PI ($p < 0.001$; Table S10), PE ($p < 0.001$; Table S10), and PS ($p = 0.002$; Table S10) showed a tendency to reduce the fatty acyl chain length (number of acyl C atoms) with increasing temperature (Fig. 4c; Table S12). The fatty acyl chain length of PC did not change significantly in the studied temperature range.

After reaching its maximum at 15–20°C, the unsaturation of PL decreased with increasing temperature, as observed for PG ($p = 0.002$; Table S10), PI ($p = 0.002$; Table S10), and PS ($p = 0.002$; Table S10) until 30°C (Fig. 4d; Table S12). In contrast, the unsaturation of PC remained similar at all temperatures studied.

The relative distribution of PC FAs from C14 to C22 (Figs. 5a, S7; Table S13) varied little with temperature. The average fatty acyl chain length was 18.8 ± 0.3 C atoms at all growth temperatures studied. Over the temperature range studied, PC was also characterized by a relatively conservative share of FA of a given chain length (average abundance C18 > C20 > C22 > C16 > C14), the dominance of polyunsaturated fatty acid (PUFA), and the relatively conservative share

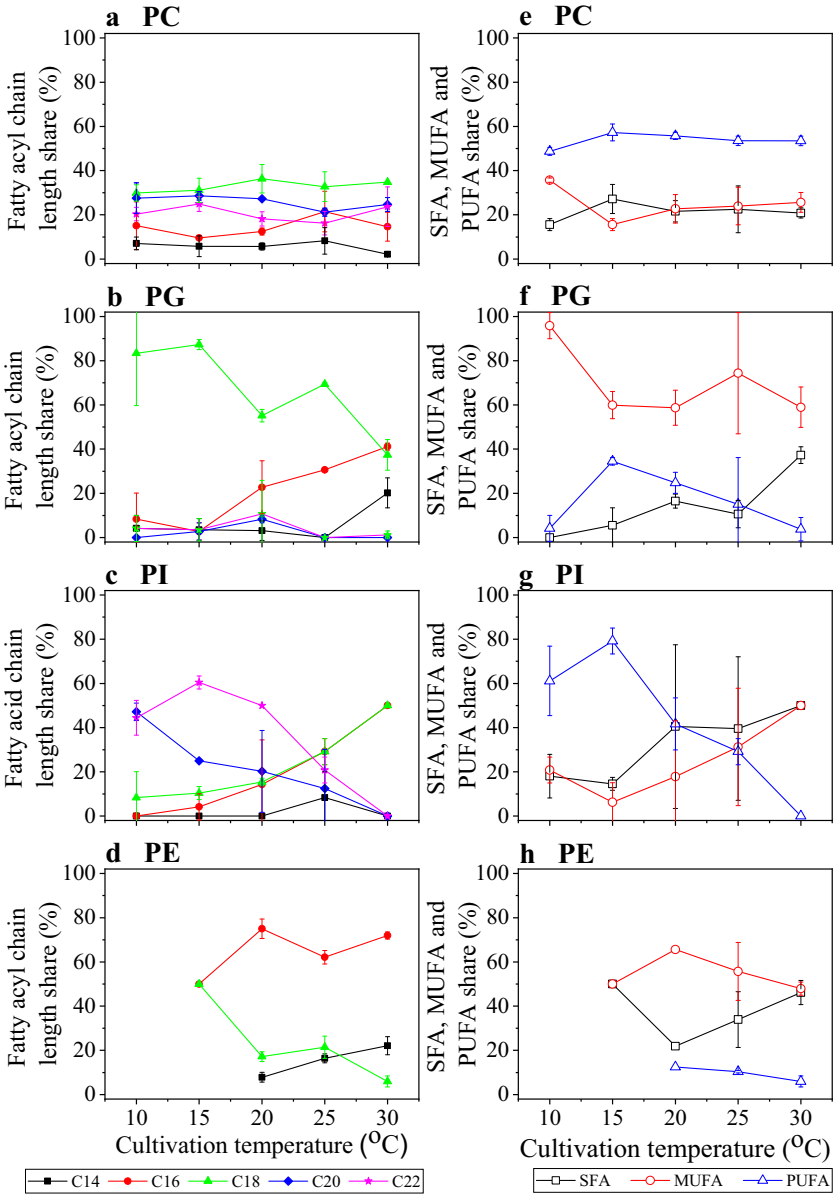

Fig. 5. Diatom *Chaetoceros pseudocurvisetus* phosphatidylcholines (PC), phosphatidylglycerols (PG), phosphatidylinositols (PI) and phosphatidylethanolamines (PE), characteristics. ((**a–d**) left panels): The average fatty acyl chain length (e.g., fatty acid with 14 carbon atoms—C14) share (%). ((**e–h**) right panels): Saturated fatty acids (SFA), monounsaturated fatty acids (MUFA), and polyunsaturated fatty acids (PUFA) share (%). Error bars are the SD of two replicates.

of PUFA, monounsaturated fatty acids (MUFA), and saturated fatty acids (SFA) (average abundance PUFA > MUFA > SFA) (Fig. 5e). The average PC unsaturation remained similar during the growth of *C. pseudocurvisetus* at all temperatures studied (double bonds 2.1 ± 0.2).

FAs C18 were most abundant in the PG lipid class (Figs. 5b, S8; Table S13). Their share decreased considerably at higher growth temperatures (from 83.3 ± 23.6% to 37.4 ± 6.9% at 30°C) ($p = 0.009$; Table S10) and were replaced mainly by C16 (from 8.3 ± 11.8% to 41.2 ± 1.6% at 30°C) ($p < 0.001$; Table S10). At all temperatures studied, the PG content was characterized by the highest share of MUFA, while the share of SFA increased significantly with increasing temperature ($p = 0.002$; Table S10) (Fig. 5f).

The PIs were characterized by the dominance of the longest (C22 [double bonds 0–6] and C20 [double bonds 0–5]) (Fig. 5c, upper panel; Fig. S9; Table S13) and the most unsaturated FA (PUFA ≥ 40%) at the optimal temperature (Novak et al. 2019), the proportion of which was significantly reduced at higher temperatures. We observed the replacement of C22 ($p < 0.001$; Table S10) and C20 ($p = 0.002$; Table S10) by C16 ($p < 0.001$; Table S10) and C18 FA ($p < 0.001$; Table S10). High growth temperature probably inhibits the biosynthesis of these FA. PI PUFA ($p = 0.001$; Table S10) were possibly replaced by MUFA ($p = 0.053$; Table S10) (Fig. 5g) at 25°C and 30°C.

We observed an increased PE occurrence at higher temperatures (Fig. 4a). The dominant FA in the PE class were C16 (Figs. 5d, S10; Table S14). PAs were not detected at the optimal growth temperature (15°C) and at 10°C, while many PA were found at higher temperatures (Fig. 4a). They were characterized by C16 FA dominance and variable PUFA, MUFA, and SFA ratios (Figs. S11, S12; Table S14). Results on PL on only few PS are presented in Figs. S11, S13.

Discussion

Long-term temporal distribution of *C. curvisetus/pseudocurvisetus* in the NW Adriatic Sea

Long-term data (over 32 years) gave us insight into population size changes, phenology, habitat, and community composition of phytoplankton populations in the NW Adriatic Sea. Phytoplankton abundance decline, both globally and in the northern Adriatic, as we detected (Figs. 1, S3a,b), was observed a decade ago and have been linked to ocean warming (Boyce et al. 2010; Marić et al. 2012). Our results show that during the period of increased seawater temperature and slightly increased salinity, indicating moderate oligotrophication, in the NW Adriatic, the contribution of *C. curvisetus/pseudocurvisetus* increased relative to the whole community, especially in spring and winter (Figs. 1e,f, S3e,f; Table S5), with summer characterized by their higher community share in the deeper layers compared to the surface layers. This suggests that *C. curvisetus/pseudocurvisetus*, unlike the majority of the accompanying phytoplankton, may have developed strategy/ies to overcome changes in the northern Adriatic. However, there is also the possibility that most other taxa are more sensitive to the observed changes, which could also explain the recent increase in the share of *C. curvisetus/pseudocurvisetus*. The high abundance and diversity of the genus *Chaetoceros* (Malviya et al. 2016) suggest that there are species within the genus that can adapt to environmental stressor/s. Indeed, Aranguren-Gassis et al. (2019) found that the marine diatom *Chaetoceros simplex* accommodate to high temperatures under the condition of high nitrogen availability. Jin and Agusti (2018) showed that *Chaetoceros tenuissimus* and *Chaetoceros* sp. may adapt to warming by using various thermal strategies. Although some species within the total accompanying community may be even better adapted compared to *C. curvisetus/pseudocurvisetus*, this was masked by the overall population response.

Parallel to the changes in the NW Adriatic, *C. curvisetus/pseudocurvisetus* changed the timing of high abundance and blooms in the surface layers (Fig. 2). The main difference in the surface layer is an alteration from bimodal in the first period to unimodal blooming in the second period, probably due to the lower possibility of blooming at higher temperatures that prevailed in August and October in the second period. We assume that the reason for this is the failure of blooming at higher temperatures. Changes in phenology (time of blooming) can lead to trophic level mismatch with a consequence for ecosystem functioning (Edwards and Richardson 2004).

The recent occurrence of *C. curvisetus/pseudocurvisetus* at higher 10-d temperature and salinity anomalies (Fig. 3; Tables S7, S8), suggests that they have accommodated to the new seawater conditions, the warmer and moderately oligotrophic NW Adriatic. A number of indirect changes caused by global change, such as altered light availability (Wiltshire et al. 2015), altered trophic interactions (Horn et al. 2020), and so forth, could contribute to the successful adaptation of *C. curvisetus/pseudocurvisetus*. We found that the accommodation strategies of *C. curvisetus/pseudocurvisetus* involve a shift of microhabitat to deeper, colder layers, probably to avoid high surface temperatures, as observed during the summer months when their community share is higher in the deeper than surface layer (Table S5). Since the Secchi disk depth in the NW Adriatic is about 10 m (Justić 1988), we can hypothesize that *C. curvisetus/pseudocurvisetus* shift to deeper layers is enabled by adjusting the amount and/or pigment structure, which have direct properties on photosynthetic efficiency (Churilova et al. 2019). Also, cell abundances > 10^5 cell L^{-1}, which were often found in the surface layer throughout the year in the first period, were much rarer in the second period and limited to spring and winter. The shift in phytoplankton community composition is generally due to the ability of the various phytoplankton taxa to adapt to temperature increases in an evolutionary sense (Huertas et al. 2011).

The long-term studies that address the impact of global warming on phytoplankton populations in the seas and oceans are very important to the marine science research community. Wiltshire and Manly (2004) reported that warming of the Helgoland Roads (North Sea) by 1.1°C, during 1962–2002 caused a shift in phytoplankton succession. More recent studies report significant changes in phytoplankton abundance and composition in the NE subarctic Pacific Ocean as a result of sea surface warming (Peña et al. 2019). Over a period from 1931 to 2019, the relative ratio of warm- to cold-water phytoplankton species increased at a coastal station off Sydney, Australia in the Pacific Ocean (Ajani et al. 2020). Geological data on the response of marine phytoplankton to warming are also informative. Studies of the response of diatom phytoplankton to warming in the middle Eocene revealed that the dominance of cosmopolitan species of the diatom genus *Triceratium* before warming was replaced by a more diverse assemblage after warming (Renaudie et al. 2010).

C. pseudocurvisetus phospholipidomics

The sea surface warming may seriously impair the central role of eukaryotic phytoplankton in organic matter flux to both higher trophic levels and deep waters (Falkowski et al. 2004). Studying their response to warming stress is critical for predicting future changes in oceanic production and export.

In addition to temporal and/or habitat shifts, shifts were also seen in *C. curvisetus*/*pseudocurvisetus* physiology. Among changes in photosynthesis, respiration, and growth, the physiological modifications comprise changes in cell biochemistry, including lipid remodeling. PLs play a fundamental role in compartmentalizing the biochemistry of life, and serve to maintain membrane structure and function under stressful conditions.

The composition of lipid classes of diatoms varies from species to species (Volkman et al. 1989), during their life cycle (Lombardi and Wangersky 1995), and under different growth conditions (Alonso et al. 1998; Novak et al. 2019). Higher growth temperatures (25°C and 30°C) resulted in PL accumulation, suggesting that cell lipid accumulation is a heat-response mechanism (Fig. 4a). Schwenk et al. (2013) found that warm-water marine microalgae had higher lipid content than cold-water microalgae. Similarly, short-term temperature responses in the marine diatom *Thalassiosira pseudonana* resulted a significant increase in both cellular carbon (lipids are rich in carbon!) and phosphorus content (Schaum et al. 2018).

The short-term *C. pseudocurvisetus* response to high temperature included increased PL diversity (Fig. 4b; Table S4). We can speculate that *C. pseudocurvisetus* growing under favorable conditions do not require complex PL species composition, whereas diversification of PL FA composition represented a mechanism to cope with unfavorable growth temperature.

Here we found that the short-term response was different for different PLs. At the same time, some PL classes undergo similar compositional changes with an increase in temperature. In contrast to our results for PG, PI, PE, and PS, where a shortening of chain length was observed (Fig. 4c), we expected the length of PL fatty acyl chains to increase with increasing temperature to maintain membrane integrity. This is because hydrophobicity increases as the chain length increases, which inevitably leads to increased hydrophobic interactions between the PL acyl chain residues, especially the saturated ones. This would reduce thermal oscillations and thus keep the membrane intact to maintain its function. In contrast to other PL, the average PC acyl chain length remains similar at all growth temperatures (Fig. 4c). This suggests that it is important for *C. pseudocurvisetus* to maintain membrane thickness (regulated by PC fatty acyl chain length) over a wide range of temperatures. Membrane thickness may affect protein localization (Klose et al. 2013) and thus cell physiology. It appears that the PLs PG, PI, PE, and PS, unlike PC, do not play an important role in maintaining membrane thickness in *C. pseudocurvisetus* and that their FA chain shortening represents an energy and material conservation under unfavorable conditions.

The short-term response to an increase in temperature is decreased unsaturation of PG, PI, and PS (Fig. 4d). FAs 22 : 6 n-3 (eicosapentaenoic acid) and 20 : 5 n-3 (docosahexaenoic acid), omega-3 FA, decreased contribution was observed in response to global warming (Hixson and Arts 2016), indirectly affecting all aquatic ecosystems. An inverse relationship between temperature and FA unsaturation is well documented (Thompson et al. 1992). However, long-term exposure of the four diatoms (*Chaetoceros* sp., *Thalassiosira* sp., *C. tenuissimus*, and *Synedra* sp.) to high temperatures showed that some species adapt by recovering some FA essential for the higher trophic levels (Jin et al. 2020). PLs with saturated FA have a higher melting temperature range than those with unsaturated FA (Wang et al. 2016) and thus avoid membrane fluidization at high temperature. This suggests their involvement in thermal adaptation. On the other hand, increased PL saturation may increase the likelihood of carbon export to the deep ocean (Gašparović et al. 2016).

The small variation in the relative distribution of FA chain lengths, total unsaturation, and dominance of PUFA in PC (Figs. 5a,e, S7; Table S13) suggests that *C. pseudocurvisetus* invests energy to maintain the PC FA composition, probably at the expense of growth and reproduction, as these were reduced at the highest cultivation temperature, 30°C (Novak et al. 2019). We conclude that PC invariability is important for *C. pseudocurvisetus* to maintain the membrane function(s).

FAs with 18 carbon atoms are the most important for PG (Figs. 5b, S8; Table S13). The highest C18 : 1 percentage (Table S13) in the wide temperature range of *C. pseudocurvisetus* cultivation indicates the importance of this FA for the proper functioning of PG in membranes. The

unsaturation of PG is important for the PG role in photosynthetic electron transport in thylakoids, where electron flow is faster through the more fluid membrane (Siegenthaler and Murata 2004), whose fluidity is higher in the presence of unsaturated FAs.

The PI were characterized by the dominance of the longest (C22 and C20) and the most unsaturated FA (PUFA ≥ 40%) at the optimal temperature (Figs. 5c,g, S9; Table S13). We presume that very long-chain and unsaturated FA are essential for the functioning of PI, at least for the *C. pseudocurvisetus* studied. The proportion of long unsaturated FAs was significantly reduced at higher temperatures. The high growth temperature probably inhibits the biosynthesis of these FA. It appears that PI role is suppressed at high temperatures, as evidenced by a significant decrease in molecular diversity with increasing temperature (1 species was detected at 30°C).

On the other hand, we observed an increased PE occurrence at higher temperatures (Fig. 4b). This could be explained by the role of PE in reducing membrane fluidization at higher temperatures. The lipid polar group influences lipid melting phase transition temperature (Cevc 1987). The temperature at which the hydrocarbon membrane core begins to fluidize is higher for PE than for PC with the same FA composition. Low PE saturation (Figs. 5h, S10; Table S14) also contributes to the thermal stability of the membrane.

PAs are signaling and regulatory molecules in phytoplankton cells and precursors in other PL biosynthesis (Khozin-Goldberg 2016). Since PA was detected only at higher temperatures (20–30°C) (Fig. 4b), we can assume that PA served mainly for the synthesis of PC and PG, whose diversity increased at the highest temperatures. At the same time, PA could be released from PLs by phospholipase D activity (Beligni et al. 2015). The increased diversity of PA could be an indication of stress in *C. pseudocurvisetus*. Because only a few PS molecules were detected (Figs. 4b, S11, S13; Tables S6, S9), we cannot draw any conclusions about this PL class.

Our results suggest that the concept of FA biomarkers used to determine the composition of the major phytoplankton community, in studies to identify key processes in marine ecosystems or to study transfer from primary producers to primary consumers, likely needs to be re-evaluated in the context of global change. This will require longer-term laboratory studies of other acylglycerols and phytoplankton classes.

Summarizing considerations

C. curvisetus/*pseudocurvisetus* may employ multiple mechanisms to acclimate and adapt to alterations caused by global change. In situ observations have shown that *C. curvisetus*/*pseudocurvisetus* have changed their ecological niche in the NW Adriatic to adapt to the new conditions. At the same time, it is capable of triggering physiological mechanisms aimed at acclimation to temperature increase. It has been observed that *C. pseudocurvisetus* increases chlorophyll *a* synthesis as a result of temperature rise, which is explained by obtaining energy for physiological processes necessary for survival at high temperature (Flanjak et al. 2022). Another biochemical mechanism demonstrating the acclimation mechanism, which is elaborated in this work, is PL classes FA remodeling. The major changes in the majority of PL, caused by high temperatures, include increased diversity, shortening of FA chain lengths, and decreased FA unsaturation, changes that occur gradually with temperature rise. In contrast, the FA composition and the degree of unsaturation in PC remain approximately constant over the entire temperature range studied (10–30°C). This indicates the importance of PC in maintaining stable membrane properties, which are important for proper physiological activity.

The northern Adriatic is changing. Summer temperatures approach 30°C and occasionally exceed it. Oligotrophication has progressed. Global change is causing changes in phytoplankton composition that can have significant impact on ecosystem functioning (Di Pane et al. 2022). Different phytoplankton species respond differently to climate change, and some species will adapt better to the changes. As shown here by a cultivation experiment, *C. pseudocurvisetus* survives and reproduces even at 30°C, although it prefers lower temperatures. Thus, *C. curvisetus*/*pseudocurvisetus* alter habitat, that is, they changed the timing of high abundance and blooms in the surface layer to moderate-temperature spring months, while during the warm summer months they thrived successfully in the deeper, colder layers which was noted by their increased share in the phytoplankton community, as we observed in the NW Adriatic from 1986 to 2017.

Data availability statement

Source data used for figures are available publicly available through https://urn.nsk.hr/urn:nbn:hr:241:107649.

References

Ajani, P. A., C. H. Davies, R. S. Eriksen, and A. J. Richardson. 2020. Global warming impacts micro-phytoplankton at a long-term Pacific Ocean coastal station. Front. Mar. Sci. **7**: 576011. doi:10.3389/fmars.2020.576011

Alonso, D. L., E. L. Belarbi, J. Rodriguez-Ruiz, C. I. Segura, and A. Gimenez. 1998. Acyl lipids of three microalgae. Phytochemistry **47**: 1473–1481. doi:10.1016/S0031-9422(97)01080-7

Aranguren-Gassis, M., C. T. Kremer, C. A. Klausmeier, and E. Litchman. 2019. Nitrogen limitation inhibits marine diatom adaptation to high temperatures. Ecol. Lett. **22**: 1860–1869. doi:10.1111/ele.13378

Artamonova, E. Y., J. B. Svenning, T. Vasskog, E. Hansen, and H. C. Eilertsen. 2017. Analysis of phospholipids and neutral lipids in three common northern cold water diatoms: *Coscinodiscus concinnus*, *Porosira glacialis*, *and Chaetoceros socialis*, by ultra–high performance liquid chromatography–

mass spectrometry. J. Appl. Phycol. **29**: 1241–1249. doi:10.1007/s10811-017-1055-0

Arts, M. T., R. G. Ackman, and B. J. Holub. 2001. "Essential fatty acids" in aquatic ecosystems, a crucial link between diet and human health and evolution. Can. J. Fish. Aquat. Sci. **58**: 122–137. doi:10.1139/f00-224

Bates, D., M. Maechler, B. Bolker, and S. Walker. 2015. Fitting linear mixed-effects models using *lme4*. J. Stat. Softw. **67**: 1–48. doi:10.18637/jss.v067.i01

Bates, D.M and W.N. Venables. 2020. Regression spline functions and classes (Package: *splines*, built R 3.6.3).

Behrenfeld, M. J., and others. 2006. Climate-driven trends in contemporary ocean productivity. Nature **444**: 752–755. doi:10.1038/nature05317

Beligni, M. V., C. Bagnato, M. B. Prados, H. Bondino, A. M. Laxalt, T. Munnik, and A. Ten Have. 2015. The diversity of algal phospholipase D homologs revealed by biocomputational analysis. J. Phycol. **51**: 943–962. doi:10.1111/jpy.12334

Bligh, E. G., and W. J. Dyer. 1959. A rapid method of total lipid extraction and purification. Can. J. Biochem. Phys. **37**: 911–917. doi:10.1139/o59-099

Bosak, S., J. Godrijan, and T. Šilović. 2016. Dynamics of the marine planktonic diatom family Chaetocerotaceae in a Mediterranean coastal zone. Estuar. Coast. Shelf Sci. **180**: 69–81. doi:10.1016/j.ecss.2016.06.026

Boyce, D. G., M. R. Lewis, and B. Worm. 2010. Global phytoplankton decline over the past century. Nature **466**: 591–596. doi:10.1038/nature09268

Busseni, G., and others. 2020. Large scale patterns of marine diatom richness: Drivers and trends in a changing ocean. Glob. Ecol. Biogeogr. **29**: 1915–1928. doi:10.1111/geb.13161

Cevc, G. 1987. How membrane chain melting properties are regulated by the polar surface of the lipid bilayer. Biochemistry **26**: 6305–6310. doi:10.1021/bi00394a002

Churilova, T., and others. 2019. Phytoplankton light absorption in the deep chlorophyll maximum layer of the Black Sea. Eur. J. Remote Sens. **52**: 123–136. doi:10.1080/22797254.2018.1533389

Cozzi, S., and M. Giani. 2011. River water and nutrient discharges in the Northern Adriatic Sea: Current importance and long term changes. Cont. Shelf Res. **31**: 1881–1893. doi:10.1016/j.csr.2011.08.010

Di Pane, J., K. H. Wiltshire, M. McLean, M. Boersma, and C. L. Meunier. 2022. Environmentally induced functional shifts in phytoplankton and their potential consequences for ecosystem functioning. Glob. Change Biol. **28**: 2804–2819. doi:10.1111/gcb.16098

Edwards, M., and A. J. Richardson. 2004. Impact of climate change on marine pelagic phenology and trophic mismatch. Nature **430**: 881–884. doi:10.1038/nature02808

Falkowski, P. G., M. E. Katz, A. H. Knoll, A. Quigg, J. A. Raven, O. Schofield, and F. J. R. Taylor. 2004. The evolution of modern eukaryotic phytoplankton. Science **305**: 354–360. doi:10.1126/science.1095964

Field, C. B., M. J. Behrenfeld, J. T. Randerson, and P. G. Falkowski. 1998. Primary production of the biosphere: Integrating terrestrial and oceanic components. Science **281**: 237–240. doi:10.1126/science.281.5374.237

Filiz, N., and others. 2020. Phytoplankton community response to nutrients, temperatures, and a heat wave in shallow lakes: An experimental approach. Water **12**: 3394. doi:10.3390/w12123394

Flanjak, L., I. Vrana, A. Cvitešić Kušan, J. Godrijan, T. Novak, A. Penezić, and B. Gašparović. 2022. The effects of high temperatures and nitrogen availability on the growth and composition of the marine diatom *Chaetoceros pseudocurvisetus*. J. Exp. Bot. **73**: 4250–4265. doi:10.1093/jxb/erac145

Gašparović, B. 2012. Decreased production of surface–active organic substances as a consequence of the oligotrophication in the northern Adriatic Sea. Estuar. Coast. Shelf Sci. **115**: 33–39. doi:10.1016/j.ecss.2012.02.004

Gašparović, B., S. P. Kazazić, A. Cvitešić, A. Penezić, and S. Frka. 2015. Improved separation and analysis of glycolipids by Iatroscan thin–layer chromatography–flame ionization detection. J. Chromtogr. A **1409**: 259–267. doi:10.1016/j.chroma.2015.07.047

Gašparović, B., A. Penezić, R. S. Lampitt, N. Sudasinghe, and T. Schaub. 2016. Free fatty acids, tri-, di- and monoacylglycerol production and depth-related cycling in the Northeast Atlantic. Mar. Chem. **186**: 101–109. doi:10.1016/j.marchem.2016.09.002

Graves, S., H.-P. Piepho, L. Selzer, and S. Dorai-Raj. 2019. *multcompView*: Visualizations of Paired Comparisons. R package version 0.1-8. https://CRAN.R-project.org/package=multcompView

Grilli, F., and others. 2020. Seasonal and interannual trends of oceanographic parameters over 40 years in the northern Adriatic Sea in relation to nutrient loadings using the EMODnet chemistry data portal. Water **12**: 2280. doi:10.3390/w12082280

Grosjean P., and F. Ibanez. 2018. *pastecs*: Package for Analysis of Space-Time Ecological Series. R package version 1.3.21. https://CRAN.R-project.org/package=pastecs

Guillard, R. R. L. 1975. Culture of phytoplankton for feeding marine invertebrates, p. 26–60. *In* W. L. Smith and M. H. Chanley [eds.], Culture of marine invertebrate animals. Springer. doi:10.1007/978-1-4615-8714-9_3

Guschina, I. A., and J. L. Harwood. 2009. Algal lipids and effect of the environment on their biochemistry, p. 1–24. *In* M. Kainz, M. Brett, and M. Arts [eds.], Lipids in aquatic ecosystems. Springer. doi:10.1007/978-0-387-89366-2_1

Hixson, S. M., and M. T. Arts. 2016. Climate warming is predicted to reduce omega-3, long-chain, polyunsaturated fatty acid production in phytoplankton. Glob. Change Biol. **22**: 2744–2755. doi:10.1111/gcb.13295

Holthuis, J. C. M., and A. K. Menon. 2014. Lipid landscapes and pipelines in membrane homeostasis. Nature **510**: 48–57. doi:10.1038/nature13474

Horn, H. G., M. Boersma, J. Garzke, U. Sommer, and N. Aberle. 2020. High CO_2 and warming affect microzooplankton food web dynamics in a Baltic Sea summer plankton community. Mar. Biol. **167**: 69. doi:10.1007/s00227-020-03683-0

Huertas, I. E., M. Rouco, V. Lopez–Rodas, and E. Costas. 2011. Warming will affect phytoplankton differently: Evidence through a mechanistic approach. Proc. Biol. Sci. **278**: 3534–3543. doi:10.1098/rspb.2011.0160

Ivančić, I., J. Godrijan, M. Pfannkuchen, D. Marić, B. Gašparović, T. Đakovac, and M. Najdek. 2012. Survival mechanisms of phytoplankton in conditions of stratification induced deprivation of orthophosphate: Northern Adriatic case study. Limnol. Oceanogr. **57**: 1721–1731. doi:10.4319/lo.2012.57.6.1721

Jin, P., and S. Agusti. 2018. Fast adaptation of tropical diatoms to increased warming with trade-offs. Sci. Rep. **8**: 17771. doi:10.1038/s41598-018-36091-y

Jin, P., G. Gonzàlez, and S. Agustí. 2020. Long-term exposure to increasing temperature can offset predicted losses in marine food quality (fatty acids) caused by ocean warming. Evol. Appl. **13**: 2497–2506. doi:10.1111/eva.13059

Justić, D. 1988. Trend in the transparency of the northern Adriatic Sea 1911–1982. Mar. Poll. Bull. **19**: 32–35. doi:10.1016/0025-326X(88)90751-5

Khozin-Goldberg, I. 2016. Lipid metabolism in microalgae, p. 413–484. *In* M. Borowitzka, J. Beardall, and J. Raven [eds.], The physiology of microalgae. Developments in applied phycology. Springer. doi:10.1007/978-3-319-24945-2_18

Klose, C., M. A. Surma, and K. Simons. 2013. Organellar lipidomics—Background and perspectives. Curr. Opin. Cell Biol. **25**: 406–413. doi:10.1016/j.ceb.2013.03.005

Lombardi, A., and P. J. Wangersky. 1995. Particulate lipid class composition of 3 marine phytoplankters *Chaetoceros gracilis*, *Isochrysis galbana* (Tahiti) and *Dunaliella tertiolecta* grown in batch culture. Hydrobiologia **306**: 1–6. doi:10.1007/BF00007853

Mair, P., and R. Wilcox. 2020. Robust statistical methods in r using the WRS2 package. Behav. Res. Methods **52**: 464–488. doi:10.3758/s13428-019-01246-w

Malviya, S., and others. 2016. Insights into global diatom distribution and diversity in the world's ocean. Proc. Natl. Acad. Sci. USA **113**: E1516–E1525. doi:10.1073/pnas.1509523113

Marić, D., R. Kraus, J. Godrijan, N. Supić, T. Djakovac, and R. Precali. 2012. Phytoplankton response to climate and anthropogenic influences in the north-eastern Adriatic during the last four decades. Estuar. Coast. Shelf Sci. **115**: 98–112. doi:10.1016/j.ecss.2012.02.003

Mason, J. G., M. A. Rudd, and L. B. Crowder. 2017. Ocean research priorities: Similarities and differences among scientists, policymakers, and fishermen in the United States. Bioscience **67**: 418–428. doi:10.1093/biosci/biw172

Nelson, D. M., P. Treguer, M. A. Brzezinski, A. Leynaert, and B. Queguiner. 1995. Production and dissolution of biogenic silica in the ocean: Revised global estimates, comparison with regional data and relationship to biogenic sedimentation. Glob. Biogeochem. Cycles **9**: 359–372. doi:10.1029/95GB01070

Novak, T., J. Godrijan, D. Marić Pfannkuchen, T. Djakovac, M. Mlakar, A. Baricevic, M. Smodlaka Tanković, and B. Gašparović. 2018. Enhanced dissolved lipid production as a response to the sea surface warming. J. Mar. Sys. **180**: 289–298. doi:10.1016/j.jmarsys.2018.01.006

Novak, T., J. Godrijan, D. Marić Pfannkuchen, T. Djakovac, N. Medić, I. Ivančić, M. Mlakar, and B. Gašparović. 2019. Global warming and oligotrophication lead to increased lipid production in marine phytoplankton. Sci. Total Environ. **668**: 171–183. doi:10.1016/j.scitotenv.2019.02.372

Obata, T., A. R. Fernie, and A. Nunes-Nesi. 2013. The central carbon and energy metabolism of marine diatoms. Metabolites **3**: 325–346. doi:10.3390/metabo3020325

Parrish, C. C. 1987. Separation of aquatic lipid classes by Chromarod thin-layer chromatography with measurement by Iatroscan flame ionization detection. Can. J. Fish. Aquat. Sci. **44**: 722–731. doi:10.1139/f87-087

Parrish, C. C., T. A. Abrajano, S. M. Budge, R. J. Helleur, E. D. Hudson, K. Pulchan, and C. Ramos. 2000. Lipid and phenolic biomarkers in marine ecosystems: Analysis and applications, p. 193–223. *In* P. J. Wangersky [ed.], Marine chemistry. Springer. doi:10.1007/10683826_8

Pastor, F., J. A. Valiente, and J. L. Palau. 2018. Sea surface temperature in the Mediterranean: Trends and spatial patterns (1982–2016). Pure Appl. Geophys. **175**: 4017–4029. doi:10.1007/s00024-017-1739-z

Peña, M. A., N. Nemcek, and M. Robert. 2019. Phytoplankton responses to the 2014–2016 warming anomaly in the northeast subarctic Pacific Ocean. Limnol. Oceanogr. **64**: 515–525. doi:10.1002/lno.11056

Popendorf, K. J., and others. 2011. Gradients in intact polar diacylglycerolipids across the Mediterranean Sea are related to phosphate availability. Biogeosciences **8**: 3733–3745. doi:10.5194/bg-8-3733-2011

R Core Team (2020). R: A language and environment for statistical computing. R Foundation for Statistical Computing, Vienna, Austria. https://www.R-project.org/

Renaudie, J., T. Danelian, S. Saint Martin, L. Le Callonnec, and L. Tribovillard. 2010. Siliceous phytoplankton response to a Middle Eocene warming event recorded in the tropical Atlantic (Demerara Rise, ODP site 1260A). Palaeogeogr. Palaeocl. Palaeoecol. **286**: 121–134. doi:10.1016/j.palaeo.2009.12.004

Richardson, A. J. 2008. In hot water: Zooplankton and climate change. ICES J. Mar. Sci. **65**: 279–295. doi:10.1093/icesjms/fsn028

Schaum, C.-E., A. Buckling, N. Smirnoff, D. J. Studholme, and G. Yvon-Durocher. 2018. Environmental fluctuations accelerate molecular evolution of thermal tolerance in a marine diatom. Nat. Commun. **9**: 1719. doi:10.1038/s41467-018-03906-5

Schiller, J. 1937. Dinoflagellatae (Peridineae). Akademische Verlagsgesellschaft.

Schwenk, D., J. Seppälä, K. Spilling, A. Virkki, T. Tamminen, K.-M. Oksman-Caldentey, and H. Rischer. 2013. Lipid content in 19 brackish and marine microalgae: Influence of growth phase, salinity and temperature. Aquat. Ecol. **47**: 415–424. doi:10.1007/s10452-013-9454-z

Sieburth, J. M., V. Smetacek, and J. Lenz. 1978. Pelagic ecosystem structure: Heterotrophic compartments of the plankton and their relationship to plankton size–fractions. Limnol. Oceanogr. **23**: 1256–1263. doi:10.4319/lo.1978.23.6.1256

Siegenthaler, P.-A., and N. Murata. 2004. Lipids in photosynthesis: Structure, function and genetics. Springer.

Solidoro, C., and others. 2009. Current state, scales of variability and decadal trends of biogeochemical properties in the northern Adriatic Sea. J. Geophys. Res.: Oceans **114**: C07S91. doi:10.1029/2008JC004838

Supić, N., M. Orlić, and D. Degobbis. 2000. Istrian coastal countercurrent and its year-to-year variability. Estuar. Coast. Shelf Sci. **51**: 385–397. doi:10.1006/ecss.2000.0681

Thompson, P. A., M. X. Guo, P. J. Harrison, and J. N. C. Whyte. 1992. Effects of variation in temperature. II. On the fatty acid composition of 8 species of marine phytoplankton. J. Phycol. **28**: 488–497. doi:10.1111/j.0022-3646.1992.00488.x

Tomas, C. R. 1995. Identifying marine phytoplankton. Academic Press.

Utermöhl, H. 1958. Zur Vervollkommnung der quantitativen Phytoplankton Methodik. Mitt. Int. Ver. Theor. Angew. Limnol. **9**: 1–38. doi:10.1080/05384680.1958.11904091

van Meer, G., D. R. Voelker, and G. W. Feigenson. 2008. Membrane lipids: Where they are and how they behave. Nat. Rev. Mol. Cell Biol. **9**: 112–124. doi:10.1038/nrm2330

Volkman, J. K., S. W. Jeffrey, P. D. Nichols, G. I. Rogers, and C. D. Garland. 1989. Fatty acid and lipid composition of 10 species of microalgae used in mariculture. J. Exp. Mar. Biol. Ecol. **128**: 219–240. doi:10.1016/0022-0981(89)90029-4

Wang, T., X. Wang, and X. Wang. 2016. Effects of lipid structure changed by interesterification on melting property and lipemia. Lipids **51**: 1115–1126. doi:10.1007/s11745-016-4184-3

Wickham, H. 2016. *ggplot2*: Elegant graphics for data analysis. Springer-Verlag.

Wilcox, R. R. 2012. Introduction to robust estimation and hypothesis testing, 3rd ed. Elsevier.

Wiltshire, K. H., and B. F. J. Manly. 2004. The warming trend at Helgoland roads, North Sea: Phytoplankton response. Helgoland Mar. Res. **58**: 269–273. doi:10.1007/s10152-004-0196-0

Wiltshire, K. H., M. Boersma, K. Carstens, A. C. Kraberg, S. Peters, and M. Scharfe. 2015. Control of phytoplankton in a shelf sea: Determination of the main drivers based on the Helgoland roads time series. J. Sea Res. **105**: 42–52. doi:10.1016/j.seares.2015.06.022

Acknowledgments

This work was funded by the grants from the Croatian Science Foundation under the projects IP-11-2013-8607, UIP 2020-2102-7868 and UIP-2014-2109-6563. The authors would like to thank the crew of the RV "Vila Velebita" for their help in sampling. We thank Dr. Martin Lončarić for the radiometric measurements of spectral irradiance. We also thank Dr. Igor Tomažić for providing satellite-derived chlorophyll *a* image for the northern Adriatic Sea.

Conflict of Interest

None declared.

Submitted 11 February 2022
Revised 25 June 2022
Accepted 15 December 2022

Associate editor: Maarten Boersma